Trace and Minor Elements in Anhydrite and Halite, Supai Formation (Permian), East-Central Arizona

Walter E. Dean
Annie Liu Tung
Department of Geology
Syracuse University
Syracuse, New York 13210

ABSTRACT

Trace and minor concentrations of Ca, Mg, Na, Mn, Sr, Fe, and K were studied in 159 samples of halite and anhydrite from two cores of the Supai Formation. In general, there are few significant differences in element concentrations between cores which might reflect systematic variations in water chemistry within the depositional basin. Ranking of mean concentrations for individual beds provides reliable stratigraphic correlations between cores. Fe and Mn are the best elements for stratigraphic correlation of anhydrite, whereas Ca is the only element in halite which correlates between cores.

In one halite bed of sufficient thickness to provide enough samples to study within-bed variations, K, Ca, Mg, and Mn increase upward within the bed, probably in response to increasing salinity. Fe concentrations within this bed are relatively constant suggesting that factors controlling co-precipitation of Fe with halite remained relatively constant during deposition of the bed.

For both halite and anhydrite, the strongest statistical correlations between elements were between K, Mg, and Mn. Weaker correlations between Fe, K, and Mg also occur, especially in anhydrite.

INTRODUCTION

The Supai Formation of Middle Permian age consists of a sequence of interbedded redbeds, evaporites, and marine limestone which underlies most of the region between the Grand Canyon and western New Mexico. The redbeds have been interpreted as a deltaic complex derived from the Defiance Uplift along the Arizona-New Mexico border (Winters, 1963). Evaporites are found mainly in the Upper Supai in the Holbrook Basin of east-central Arizona near the southern edge of the Colorado Plateau. Figure 1, a southwest to northeast cross section from

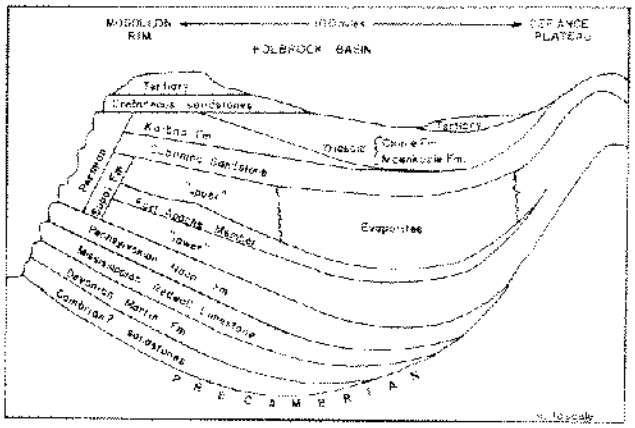

Figure 1. Diagrammatic SW-NE geologic section in east-central Arizona from Mogollon Rim to Defiance Plateau (*from* Peirce and Gerrard, 1966).

Peirce and Gerrard (1966), shows the Holbrook Basin as a structural low between the Mogollon Rim to the southwest and the Defiance Uplift to the northeast. Within the Holbrook Basin, the Upper Supai ranges in thickness from 450 to 1300 feet (137 to 397 meters), with a maximum thickness in the subsurface near Holbrook, Arizona (Peirce and Gerrard, 1966). The evaporites of the Upper Supai, mostly halite and anhydrite with some sylvite, have a cumulative thickness of up to 485 feet (148 meters) and underlie an area of about 2300 square miles (5960 square km) (Peirce and Gerrard, 1966). The approximate margin of halite in the Upper Supai is shown in Figure 2.

Figure 2 shows the locations of the two cores used for this study. These cores consist mainly of sandstone, shale, and dolomite interbedded with anhydrite and halite. Red clay or silt inclusions in anhydrite and halite are common, and in places anhydrite nodules occur in dolomite beds.

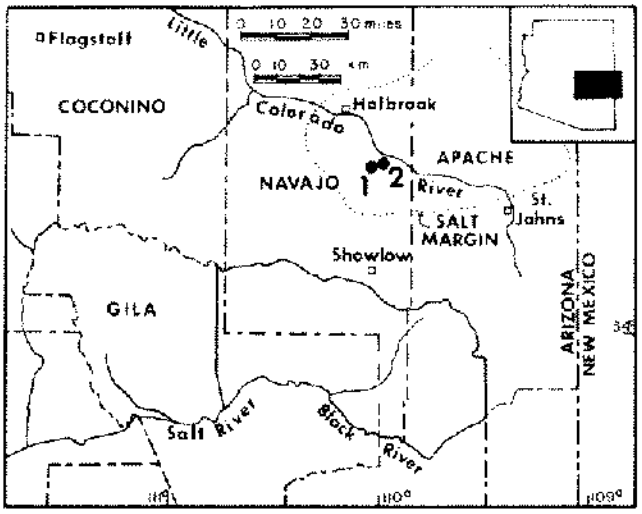

Figure 2. Map showing locations of two cores used in this study. Core 1: Scott Bros.—Strat. Test #1, Sec. 5, T. 14N., R. 22 E., Navajo County, Arizona; Core 2: Scott Bros.—Strat. Test #2, Sec. 24, T. 15 N., R. 22 E., Navajo County, Arizona. (*after* Winters, 1963; position of salt margin from Peirce and Gerrard, 1966).

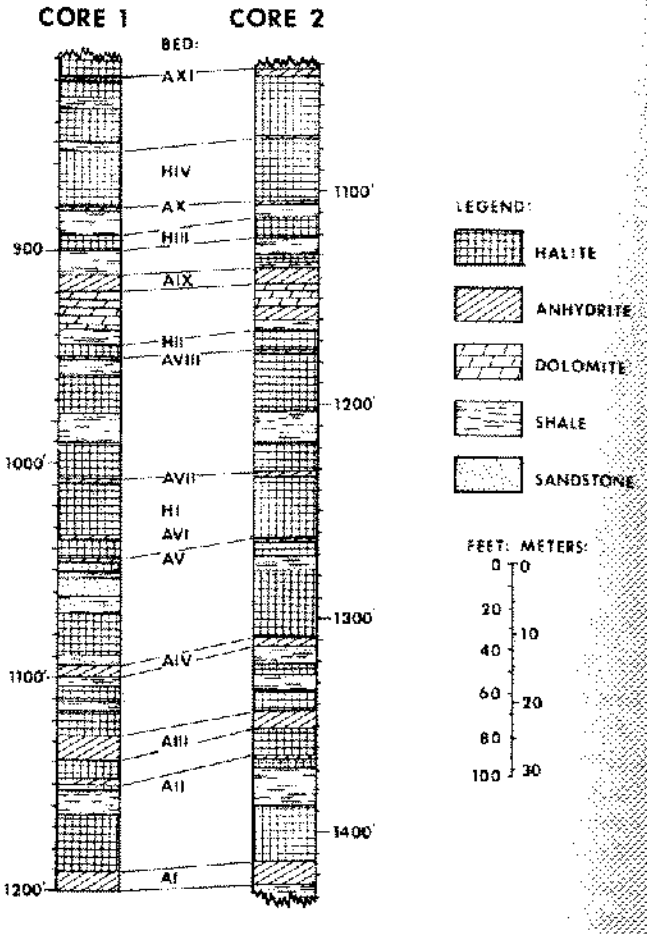

Figure 3. Generalized lithologic sections of parts of two cores used for this study (*see* Fig. 2 for locations of cores).

As can be seen in Figure 3, there is excellent stratigraphic correlation between the two cores. This correlation provides the framework for detailed investigation of vertical and lateral variations in trace and minor element concentrations. The purpose of this paper is to present results of analyses of anhydrite and halite samples collected vertically within selected correlative beds in each of the two cores. Our goals were to determine which elements, if any, might be useful for stratigraphic correlation; to see if these correlations can be related to possible regional systematic variations in water chemistry which might have existed in the depositional basin; and to determine if vertical variations within a particular core or a particular bed can be explained in terms of an evaporite salinity model which would be useful as an exploration tool.

METHODS

Because many halite and anhydrite beds in the two cores contained inclusions, mainly of clastic material, only beds which appeared to be relatively pure were sampled for analyses. Samples cut from the cores were powdered with a SPEX Mixer Mill and stored in air tight plastic vials. Powdered anhydrite samples were then dissolved in hot HCl, and powdered halite samples dissolved in distilled water. For all anhydrite samples, and most halite samples, insoluble residue was neglible. Concentrations of Sr, Mg, Fe, and Mn in anhydrite samples and Sr in halite samples were determined with a Unicam SP-90 Atomic Absorption Spectrophotometer. Concentrations of Na and K in anhydrite samples, and Ca, Mg, Na, K, Fe, and Mn in halite samples were measured with a Perkin-Elmer Model 403 Atomic Absorption Spectrophotometer. Operating parameters and total precision for each element are given in Table I. Total precision was determined by preparing one anhydrite sample ten times and analyzing the ten solutions, and therefore includes both sample preparation and analytical errors.

RESULTS

Table II summarizes the results of analyses for K, Mg, Mn, Fe, Sr, Na, and Ca in 80 anhydrite samples from seven beds, and 78 halite samples from four beds in two cores of the Supai Formation. Results of individual analyses are given in the Appendix. In general, anhydrite samples contain higher concentrations of Mg, Mn, Fe, and Sr than halite samples; concentrations of K are about the same in both minerals. Also, trace and minor element concentrations tend to be higher in core 1 for anhydrite samples and in core 2 for halite samples. These tendencies are best developed for Mn and Fe in both anhydrite and halite.

TABLE I

Instrumental parameters, detection limits, and total precision for elements analyzed by Atomic Absorption Spectrophotometry

Element	Wavelength (Å)	Range	Slit (mm) Unicam SP-90	Slit (mm) Perkin-Elmer 403	Approximate Detection Limit (ppm in dry sample)	Precision (coefficient of variation)
Ca	4227	vis	1	1	1	
Fe	2483	uv	0.3	0.3	2	±11.2%
K	7665	vis	0.3	1	1	±12.2%
Mg	2852	uv	0.3	3	0.1	± 2.3%
Mn	2795	uv	1	1	0.2	±15.6%
Na	5890	vis	–	1	1	± 3.8%
Sr	4607	vis	0.3	1	100	±13.9%

TABLE II

Means, ranges, and F-ratios for K, Mg, Mn, Fe, Sr, Na, and Ca concentrations in anhydrite and halite beds of the Supai Formation (MS1: variance between correlative beds; MS2: variance within beds; N1: number of samples from Core 1; N2: number of samples from core 2; *: F-ratios significant at the 90% confidence level).

K (PPM)

	CORE 1		CORE 2						
Bed	Mean	Range	Mean	Range	F-ratio	MS1	MS2	N1	N2
AXI	255	173 - 338	208	186 - 221	1.30	3.73×10^3	2.86×10^3	4	3
AX	343	324 - 361	259	228 - 305	6.36*	8.40×10^3	1.31×10^3	2	3
AVIII	409	247 - 571	549	237 - 862	0.16	1.97×10^4	1.24×10^5	2	2
AVII	398	269 - 519	403	250 - 594	0.00	4.67×10	1.89×10^4	3	4
AIV	325	242 - 389	281	221 - 352	1.05	3.80×10^3	3.62×10^3	4	4
AIII	379	186 - 972	380	317 - 746	0.00	7.49×10	4.00×10^4	8	9
AI	342	267 - 525	430	269 - 1578	0.22	2.60×10^4	1.17×10^5	5	10
HIV	406	285 - 465	653	290 - 1742	3.94*	4.68×10^5	1.19×10^5	15	21
HIII	322	292 - 354	315	258 - 349	0.09	9.60×10	1.12×10^2	3	5
HII	291	166 - 349	347	199 - 481	2.46	6.97×10^3	8.30×10	9	15
HI	309	239 - 346	472	378 - 515	47.48*	8.60×10^4	1.81×10^3	6	7
				Total	1.20	1.24×10^4	9.90×10^3		

Mg (PPM)

AXI	2422	956 - 5900	2328	553 - 5020	0.00	1.50×10^4	5.50×10^6	4	3
AX	2881	1501 - 4262	302	200 - 406	6.25*	7.98×10^6	1.28×10^6	2	3
AVIII	7268	2705 - 11831	4724	2150 - 7299	0.23	6.47×10^6	2.74×10^7	2	2
AVII	7444	507 - 12474	5752	1002 - 10684	0.20	4.92×10^7	2.49×10^7	3	4
AIV	1047	556 - 21169	7578	203 - 15051	0.25	1.68×10^7	6.66×10^7	4	4
AIII	5361	956 - 18349	8856	4536 - 16360	2.10	5.17×10^7	2.46×10^7	8	9
AI	10622	3232 - 35491	5903	965 - 23511	0.84	7.74×10^7	9.21×10^7	5	10
HIV	59	<0.1 - 170	658	<0.1 - 3484	3.98*	2.74×10^6	6.88×10^5	15	21
HIII	25	15 - 36	16	6 - 27	1.76	1.45×10^2	8.27×10	3	5
HII	14	<0.1 - 102	11	<0.1 - 32	0.08	4.22×10	4.87×10^2	9	15
HI	13	<0.1 - 40	18	<0.1 - 52	0.25	7.15×10	2.87×10^2	6	7
				Total	0.35	5.05×10^6	1.45×10^7		

TABLE II (Continued)

Mn (PPM)

Bed	CORE 1 Mean	CORE 1 Range	CORE 2 Mean	CORE 2 Range	F-ratio	MS1	MS2	N1	N2
AXI	11.0	6.5 - 15.5	11.9	4.5 - 24.1	0.03	1.55	5.49 X 10	4	3
AX	12.8	10.4 - 15.1	6.0	6.0 - 6.0	13.69*	5.15 X 10	3.76	2	3
AVIII	107.0	44.1 - 169.8	66.0	40.0 - 92.0	0.36	1.68×10^3	4.63×10^3	2	2
AVII	33.0	27.4 - 40.5	23.4	11.0 - 29.4	2.61	1.61×10^2	6.16 X 10	3	4
AIV	148.6	9.1 - 277.7	77.4	9.1 - 158.1	0.93	1.01×10^4	1.09×10^4	4	4
AIII	22.9	10.1 - 44.7	24.5	7.7 - 41.9	0.05	1.02 X 10	2.16×10^2	8	9
AI	80.5	13.1 - 249.6	60.7	9.1 - 329.7	0.14	1.31×10^3	9.15×10^3	5	10
HIV	1.1	0.1 - 1.7	2.7	0.7 - 10.0	4.19*	2.01×10^2	4.87	15	21
HIII	0.9	0.8 - 1.0	1.1	0.5 - 1.8	0.61	0.09	0.15	3	5
HII	0.9	0.5 - 1.5	1.6	1.1 - 2.8	11.14*	2.09	0.19	9	15
HI	0.8	0.5 - 1.3	2.6	1.2 - 5.5	9.68*	1.02 X 10	1.06	6	7
				Total	0.53	9.11×10^2	1.71×10^3		

Fe (PPM)

AXI	266	110 - 590	115	100 - 130	1.26	3.90×10^4	3.08×10^4	4	3
AX	448	398 - 499	144	85 - 203	27.70*	1.11×10^5	4.01×10^3	2	3
AVIII	425	250 - 699	674	85 - 1264	0.10	3.99×10^4	3.98×10^5	2	2
AVII	1152	557 - 1673	945	200 - 1869	0.18	7.37×10^4	4.12×10^5	3	4
AIV	274	211 - 337	213	167 - 285	2.34	7.41×10^3	3.17×10^3	4	4
AIII	773	211 - 2236	835	412 - 2522	0.04	1.64×10^4	4.44×10^5	8	9
AI	426	222 - 887	240	155 - 398	3.78*	1.15×10^5	3.03×10^4	5	10
HIV	11.0	4.6 - 14.0	11.2	8.1 - 18.2	0.03	0.16	5.32	15	21
HIII	10.2	10.1 - 10.2	10.5	8.0 - 14.3	0.07	0.26	3.52	3	5
HII	10.4	8.1 - 13.8	13.4	10.1 - 17.7	8.87*	4.80 X 10	5.42	9	15
HI	10.1	8.0 - 12.0	15.6	10.1 - 20.9	12.69	9.85 X 10	7.76	6	7
				Total	0.14	1.85×10^4	1.29×10^5		

Ca (%)

HIV	0.83	0.18 - 3.91	2.58	0.18 - 16.98	1.87	2.35×10^9	1.25×10^9	15	21
HIII	0.42	0.08 - 1.02	0.38	0.30 - 0.54	0.03	2.94×10^5	9.89×10^6	3	5
HII	1.62	0.20 - 6.91	2.95	0.14 - 18.02	0.57	1.00×10^9	1.75×10^9	9	15
HI	0.42	0.13 - 1.12	0.31	0.14 - 0.41	0.60	4.00×10^6	6.64×10^6	6	7
				Total	0.94	1.08×10^8	1.15×10^8		

Sr (PPM)

AXI	3039	753 - 4276	2058	1000 - 2918	0.86	1.65×10^6	1.92×10^6	4	3
AX	2826	2235 - 3416	1196	1087 - 1250	13.37*	3.19×10^6	2.38×10^5	2	3
AVIII	791	500 - 1081	913	700 - 1126	0.12	1.50×10^4	1.92×10^6	2	2
AVII	2086	1364 - 2495	990	911 - 1084	12.92*	1.98×10^6	1.54×10^5	3	4
AIV	844	734 - 1008	866	704 - 973	0.07	9.64×10^2	1.36×10^4	4	4
AIII	949	855 - 1089	2291	886 - 7383	1.99	7.64×10^6	3.83×10^6	8	9
AI	956	865 - 1010	884	196 - 1280	0.28	1.70×10^4	6.07×10^4	5	10
				Total	1.00	7.64×10^5	7.59×10^5		

Na (PPM)

AXI	1899	1190 - 3494	3398	1807 - 5131	2.11	3.83×10^6	1.82×10^6	4	3
AX	706	352 - 1060	406	280 - 589	1.06	1.08×10^5	1.01×10^5	2	3
AVIII	1681	554 - 2806	2406	713 - 4100	0.13	5.27×10^5	4.13×10^6	2	2
AVII	569	355 - 936	505	281 - 818	0.09	7.04×10^3	8.16×10^4	3	4
AIV	1268	1016 - 1837	2115	994 - 3418	2.42	1.43×10^6	5.92×10^5	4	4
AIII	1544	1120 - 2314	1706	1172 - 2857	0.31	1.11×10^5	3.52×10^5	8	9
AI	3265	1207 - 6639	2243	1058 - 6771	0.97	3.48×10^6	3.57×10^6	5	10
				Total	0.25	2.44×10^5	9.73×10^5		

Potassium

The concentrations of K range from 174 to 1578 ppm in anhydrite, and 166 to 1742 ppm in halite. Table II contains means, ranges, F-ratios, variance between correlative beds, and variance within beds. Although the variance of K concentrations in halite between correlative beds is generally higher than the variance within beds, the F-ratios for K concentrations are significant at the 90 percent level only for beds HI, HIV, and AX. For most anhydrite and halite beds, K concentrations are greater in core 2 than in core 1.

Magnesium

Of the elements analyzed, Mg is the most variable both within cores and between cores (Table II). On the other hand, Mg showed the least variation analytically in terms of total precision (Table I), and in terms of instrument stability during analysis. Whereas K concentrations are approximately the same in both anhydrite and halite, Mg concentrations are invariably higher in anhydrite than in halite, usually by several orders of magnitude. Mg concentrations range from 200 to 35,491 ppm (0.02 to 3.55 percent) in anhydrite, and <0.1 to 3484 ppm in halite. The F-ratios in Table II show that only two beds (AX and HIV) have significant differences in Mg concentrations between cores, and both between and within variances are generally larger than those for K.

Manganese

Concentrations of Mn range from 4.5 to 380 ppm in anhydrite and 0.1 to 10 ppm in halite. On the basis of F-ratios in Table II, mean concentrations of Mn show significant differences between cores in beds AX, HIV, HII, and HI. However, excellent correlation between cores is attained by ranking of mean concentrations for individual beds. Variance within cores is larger than variance between cores, but both are relatively small.

Iron

Concentrations of Fe, like concentrations of Mg and Mn, are invariably higher in anhydrite than in halite. Ranges in Fe concentration are 85 to 2523 ppm for anhydrite, and 5 to 20 ppm for halite. F-ratios in Table II show significant differences between cores for beds AX, AI, HII, and HI. Ranking of mean bed concentrations results in only a fair correlation between cores. Variance within cores is larger than variance between cores, and both variances are higher than Mn variances but smaller than Mg variances.

Strontium

Only 7 halite samples contained Sr concentrations >100 ppm, the detection limit with the Unicam SP-90 instrument. All 7 of these samples also contained high Ca concentrations (Appendix). Sr concentrations in Supai anhydrite samples range from 196 to 7383 ppm (0.02 to 0.74 percent). Ranking of mean values shows no correlation between cores, and F-ratios in Table II show that only beds AX and AVII have Sr differences between cores which are significant at the 90 percent level. Variances between and within cores are about the same.

Sodium

The concentration of Na ranges from 280 to 6771 ppm (0.03 to 0.68 percent) in Supai anhydrite samples. F-ratios in Table II show no significant differences in Na concentrations between cores, nor is there a correlation based on the ranking of means. Variance between cores is generally higher than variance within cores, and both are relatively high.

Calcium

The Ca concentrations in Supai halite samples show extreme variation, ranging from 0.135 to 18.0 percent. Although there are no differences between cores which are significant at the 90 percent level, ranking of mean Ca concentrations in individual beds results in perfect correlation between cores (Table II). Variances between and within cores are about the same, and both are very high.

DISCUSSION

Interelement relationships

Correlation coefficients between elements, computed using measured concentrations and logarithms of measured concentrations, are shown in Table III for anhydrite and Table IV for halite. Plots of correlations significant at

TABLE III

Correlation coefficients between K, Mg, Mn, Fe, Sr, and Na in 80 anhydrite samples from the Supai Formation based on original concentrations (A) and on logarithmic concentrations (B).

A. Based on original concentration

	K	Mg	Mn	Fe	Sr
Mg	0.5829				
Mn	0.6878	0.7940			
Fe	0.5625	0.4110	0.0904		
Sr	0.0707	−0.0220	−0.1712	0.3418	
Na	0.1916	0.0874	0.2289	−0.2256	−0.1423

B. Based on logarithmic concentration

	K	Mg	Mn	Fe	Sr
Mg	0.6597				
Mn	0.6069	0.7781			
Fe	0.7158	0.6219	0.3806		
Sr	0.0022	−0.0679	−0.2920	0.2309	
Na	−0.0807	0.1804	0.1659	0.2195	−0.2711

N = 80; 99.5% confidence level = ±0.29

Values which are significant at the 99.5 percent level are underlined.

TABLE IV

Correlation coefficients between K, Mg, Mn, Fe, and Ca in 78 halite samples from the Supai Formation based on original concentrations (A) and on logarithmic concentrations (B).

A. Based on original concentration	K	Mg	Mn	Fe
Mg	0.9397			
Mn	0.8851	0.9038		
Fe	0.1991	0.0739	0.2840	
Ca	0.2164	0.1571	0.1831	0.2090
B. Based on logarithmic concentration	**K**	**Mg**	**Mn**	**Fe**
Mg	0.6569			
Mn	0.6774	0.4294		
Fe	0.2144	−0.0009	0.3427	
Ca	0.1590	0.1091	0.3173	0.1357

N = 78; 99.5% confidence level = ±0.29

Values which are significant at the 99.5 percent level are underlined.

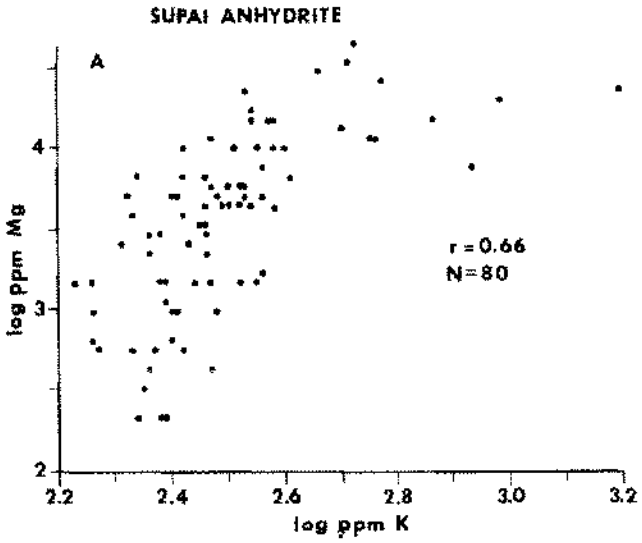

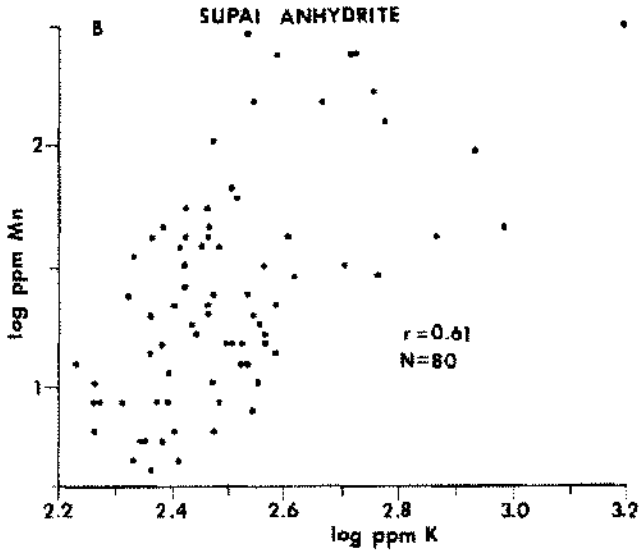

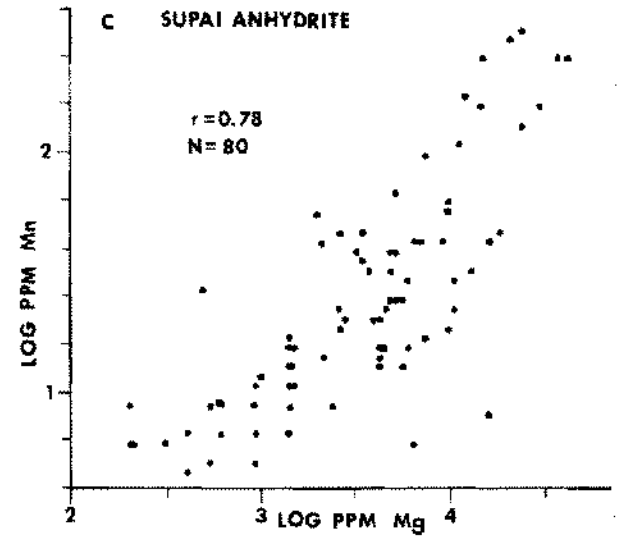

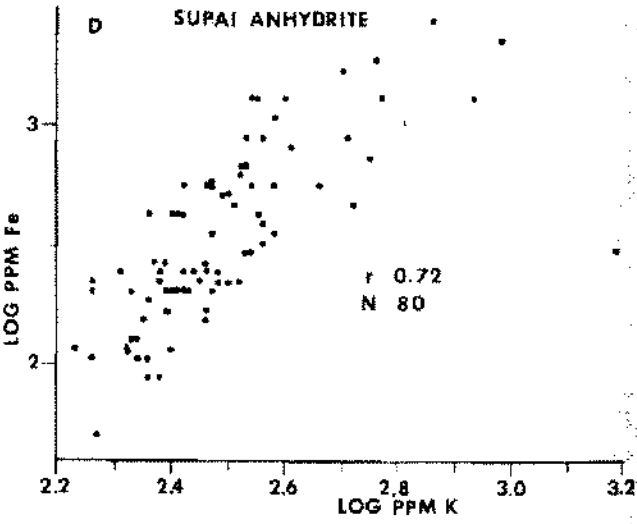

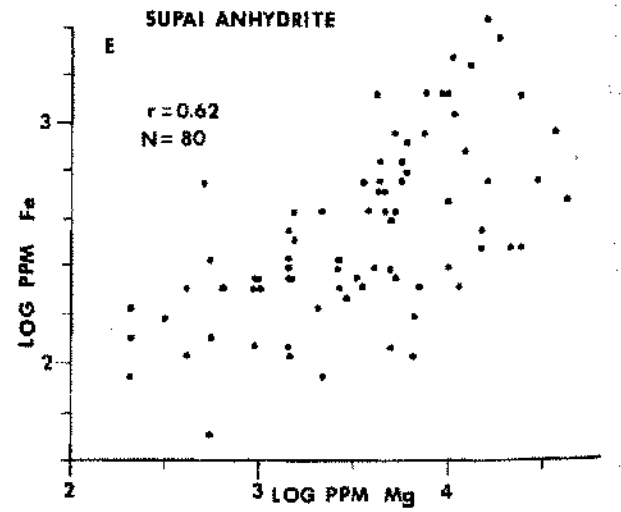

Figure 4. Scatter diagrams of concentrations of elements in Supai Anhydrite samples having significant correlations in Table III. A: log ppm Mg vs. log ppm K; B: log ppm Mn vs. log ppm K; C: log ppm Mn vs. log ppm Mg; D: log ppm Fe vs. log ppm K; E: log ppm Fe vs. log ppm Mg.

the 99.5 percent confidence level are plotted in Figures 4 and 5.

The most significant correlations, for both anhydrite and halite, are between K, Mg, and Mn, all of which show strong positive associations with each other. In anhydrite, Fe also enters this association, especially with K and Mg. From Table IV and Figure 5, note that logarithm transforms do not improve correlations between elements in halite. However, most correlations between elements in anhydrite are improved by logarithm transforms (Table III and Figure 4), suggesting that trace element incorporation processes are linear for halite but non-linear for anhydrite. In halite, logarithm transforms do strengthen positive correlations between Mn and Fe, and Mn and Ca, but these correlations are fairly weak. Except for the weak positive correlation with Mn, Ca in halite does not appear to be associated with any other elements. Unfortunately, Sr in halite samples could not be detected below 100 ppm. However, the fact that all halite samples containing >100

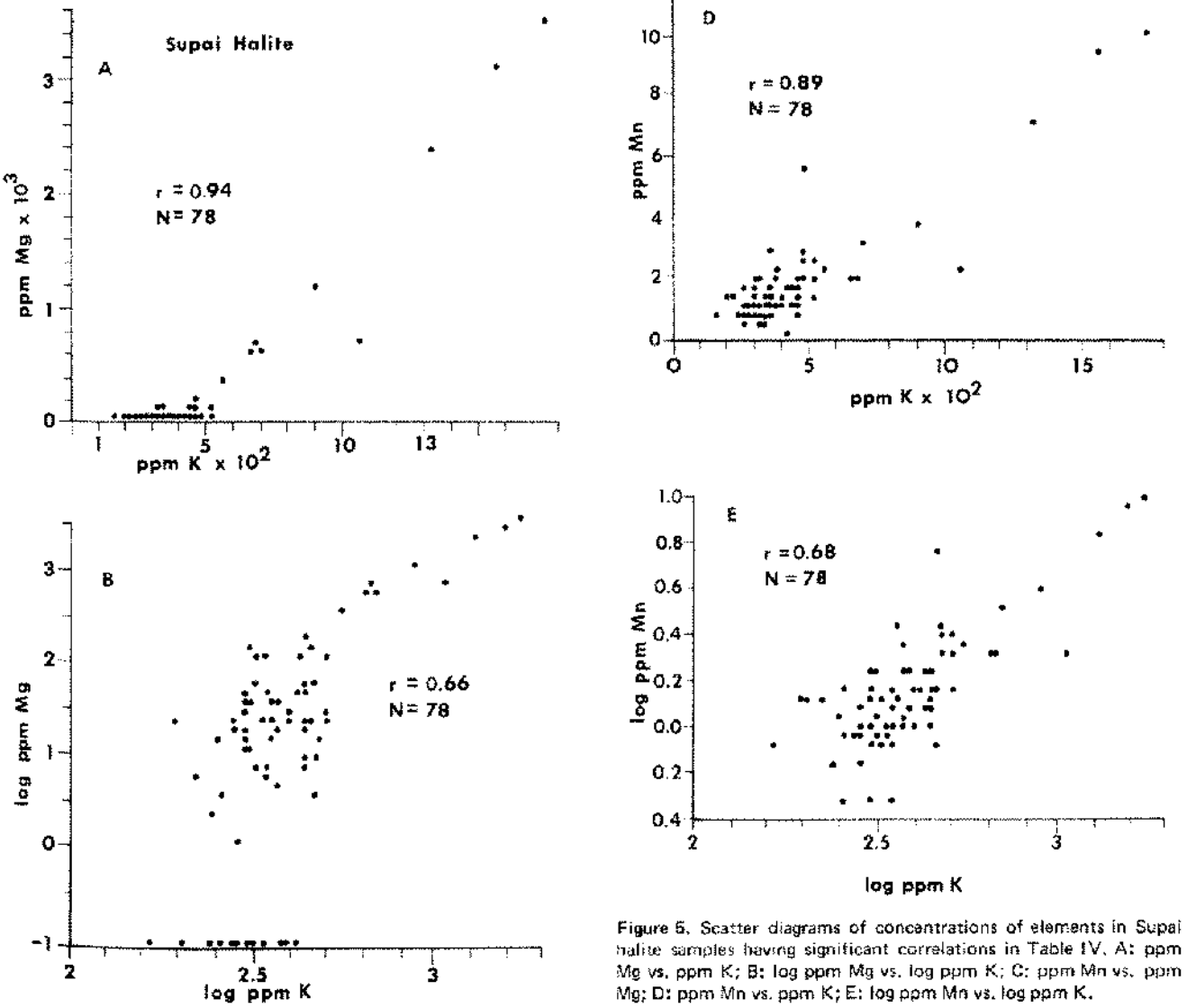

Figure 5. Scatter diagrams of concentrations of elements in Supai halite samples having significant correlations in Table IV. A: ppm Mg vs. ppm K; B: log ppm Mg vs. log ppm K; C: ppm Mn vs. ppm Mg; D: ppm Mn vs. ppm K; E: log ppm Mn vs. log ppm K.

ppm Sr invariably contain high Ca concentrations suggests that probably there is a relationship between Sr and Ca in halite. This relationship is illustrated in Figure 6, a plot of Sr vs. Ca concentrations in 9 halite samples from the Paradox Member of the Hermosa Formation, 11 halite samples from the Halite I Member of the Castile Formation (Anderson, et al., 1972), and 9 Supai halite samples containing >100 ppm Sr (7 analyses from Table A-I in the Appendix, and 2 additional analyses). The positive relationship between Sr and Ca shown in Figure 6 is what one would expect owing to the similarity of these two elements. In anhydrite, Sr shows a weak positive association with Fe, but no other correlations with Sr are significant at the 99.5 percent level. Na in anhydrite shows no significant correlations with other elements. Supai anhydrite samples differ significantly from anhydrite samples from the Castile Formation (Dean and Anderson, 1974) which show positive associations among Sr, Mg, Na, and K.

Comparison with other analyses

Mean values for concentrations of Sr, Mg, Na, K, Mn, and Fe in Supai anhydrite samples are presented in Table V along with concentrations of these elements in anhydrite samples from 10 other localities. Most of these analyses were done by us at the same time the Supai samples were analyzed. Mean values for concentrations of Ca, K, Mg, Sr, Mn, and Fe in Supai halite samples are presented in Table VI along with concentrations of these elements in halite samples from 8 other localities. Most of the additional halite analyses were taken from Moore (1960). Concentrations of K in Supai anhydrite and halite samples are in general agreement with concentrations of K in other

TABLE V

Mean concentrations of Sr, Mg, Na, K, Mn, and Fe in anhydrite samples from the Supai Formation, and in anhydrite samples from other localities. All concentrations are in parts per million (ppm).

Formation (Age)	Sr	Mg	Na	K	Mn	Fe
A. Supai (Permian)						
Mean (N = 80)	1358	6586	1626	348	45	481
Standard Deviation	±1184	±8052	±1300	±198	±67	±484
B. Castile (Permian)						
Mean (N = 510)	1107	3713	280	15		
Standard Deviation	± 675	±2679	±2679	± 17		
C. Salado (Permian)	614	615	1500	322	8	68
D. Salado (Permian)	740	59100	13100	750	93	84
E. Todilto (Triassic)						
Mean (N = 2)	1323	1205	1180	170	18	612
F. Zechstein (Permian)	660	2460	1240	560	12	320
G. Yates (Permian)	1220	1660	1240	289	9	142
H. Windsor (Triassic)	833	115	1370	245	9	20
I. Paradox (Pennsylvanian)	590	14253	1380	575	138	1388
J. Paradox (Pennsylvanian)	540	18300	670	1700	150	10300
K. Kaibab (Permian)	750	112	1080	220	8	12
L. Blaine (Permian)	100	437	1150	199	10	195
M. Blaine (Permian)	838	1300	1120	220	75	60
N. Briggs (Permian)	635	1410	1330	160	7	88

Locations: B. Means for Castile-Lower Salado varved evaporite sequence, Delaware Basin, Texas (Dean and Anderson, this volume); C. Union Anhydrite Mbr., Salado Fm., New Mexico; D. Cowden Anhydrite Mbr., Salado Fm., New Mexico (Moore, 1960); E. mean of 3 gypsum samples from the Todilto Mbr., Morrison Fm., central New Mexico; F. anhydrite from Zechstein Fm., North Sea; G. anhydrite, Yates Fm., west Texas; H. anhydrite and gypsum, Windsor Fm., Windsor, Nova Scotia; I. Paradox Mbr., Hermosa Fm., southern Utah; J. Paradox Mbr., Hermosa Fm., Delhi-Taylor No. B well, Utah (Moore, 1960); K. anhydrite, Kaibab Fm., central Arizona; L. and M. gypsum, Blaine Fm., west Texas; N. gypsum, Briggs Fm., west Texas.

TABLE VI

Mean concentrations of Ca, K, Mg, Sr, Mn, and Fe in halite samples from the Supai Formation and in halite samples from other localities. Concentrations of Ca in percent; all others in ppm.

Formation (Age)	Ca	K	Mg	Sr	Mn	Fe
A. Supai (Permian)						
Mean (N = 78)	1.68	437	195	<100	2	12
Standard Deviation	±3.34	±264	±598		±2	± 3
B. Castile (Permian)						
Mean (N = 11)	0.70	94	85	72		
Standard Deviation	±0.34	± 77	±105	±105		
C. Paradox (Pennsylvanian)						
Mean (N = 19)	0.15	635	71	45		
Standard Deviation	±0.25	±170	± 15	± 42		
D. Paradox (Pennsylvanian)	0.46	320	320	88	<0.2	8
E. Paradox (Pennsylvanian)	1.16	1600	1300	180	<0.2	15
F. Salado (Pennsylvanian)	0.13	1700	660	56	<0.2	22
G. Orchard Salt Dome	1.09	170	24	62	4	9
H. Venice Salt Dome	1.54	83	97	81	11	7
I. Venice Salt Dome	1.72	27	1000	52	20	13
J. Block 16 Salt Dome	0.46	42	110	48	1	6
K. Lower Cambrian Salt Beds	0.24	3400	42	9	<0.2	8
L. Salt Pans, Calif. (Rec.)	0.16	350	1300	74	2	5

Locations: B. 11 unpublished analyses of Halite I Member of the Castile Formation (Anderson, et al., 1972) from wells in Texas and New Mexico; C. 19 unpublished analyses of halite from three thin beds from the Paradox Member of the Hermosa Formation, Pure Oil, no. 1 Hobson well, Grand County, Utah; D. and E. Paradox Member of the Hermosa Formation, Delhi-Taylor no. 8 well, Utah (Moore, 1960); F. Salado Formation, Lea County, New Mexico (Moore, 1960); G. Duval Sulphur, Fort Bend County, Texas (Moore, 1960); H. and I. Tidewater Oil Co., Plaquemines Parish, La. (Moore, 1960); J. Humble Oil Corp., Jefferson Parish, La. (Moore, 1960); K. upper part of L.C. Salt Beds, southern Siberian Platform, U.S.S.R. (Moore, 1960); L. artificial salt pans, Leslie Salt Co., Newark, Calif. (Moore, 1960).

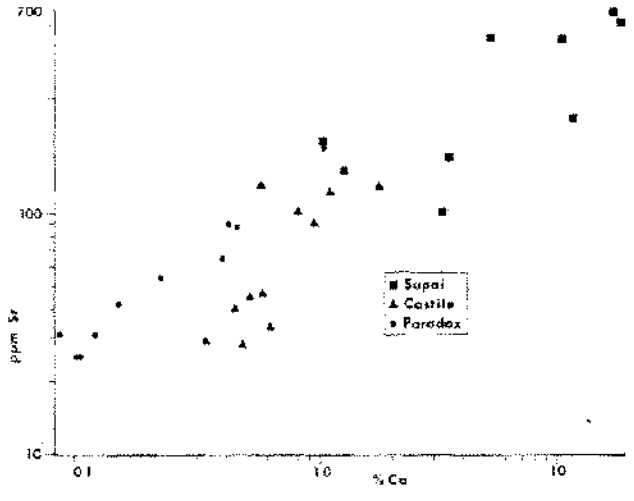

Figure 6. Scatter diagram of Sr vs. Ca concentrations in halite samples from the Paradox Member of the Hermosa Formation, the Halite I Member of the Castile Formation, and the Supai Formation.

anhydrite and halite samples. Potassium concentrations in anhydrite are relatively constant, generally varying within an order of magnitude between 100 and 1000 ppm. Potassium concentrations in halite are more variable, ranging over several orders of magnitude from several tens to several thousand ppm.

Magnesium concentrations are extremely variable in both anhydrite and halite samples. Concentrations of Mg in Supai halite samples are in general agreement with halite analyses from other localities. Magnesium variations in Supai anhydrite samples are within the range of other analyses but tend to be at the high end of this range.

Concentrations of Sr in Supai anhydrite samples are within the relatively narrow range of concentrations in other anhydrite samples but, like Mg, Sr in Supai anhydrite tends to be at the high end of this range. Most halite samples in Table 6 have Sr concentrations which are <100 ppm; only seven Supai halite samples have Sr concentrations >100 ppm.

Na concentrations in the anhydrite samples listed in Table VI are remarkably uniform, usually about 5 times K concentrations. The value of 1.31 percent Na reported from the Cowden Anhydrite Member of the Salado Formation by Moore (1960) appears to be anomalously high, and we suspect that there was probably some halite contamination. Supai analyses generally fall within the range of Na analyses from other anhydrite samples but, like Sr and Mg, tend to be at the high end of this range.

Concentrations of Fe and Mn show considerable variation in both anhydrite and halite samples. Concentrations of these two elements in Supai anhydrite and halite samples are in general agreement with concentrations in the other samples listed in Tables V and VI.

Salinity model

One of the purposes of this investigation was to determine if vertical variations in trace and minor element concentrations within a core or within an individual bed of the Supai Formation might be related to salinity variations within the depositional basin. For our salinity-concentration model, we chose the data of Morris and Dickey (1957) from Bocana de Virrila, a hypersaline estuary in northwestern Peru. The Bocana was 20 km long and 2 km wide, and had no apparent freshwater inflow. Salinities ranged from normal seawater at the mouth to 350,000 ppm in the upper reaches. Morris and Dickey found gypsum precipitating near the mouth and halite precipitating in the more saline upper reaches. Bocana de Virrila would have been an ideal natural laboratory for studying evaporite processes and the incorporation of trace and minor elements in mineral phases, but unfortunately it was destroyed in the early 1960's in an attempt to create a solar salt works. In Figure 7, we have plotted Morris and Dickey's values for Ca, Mg, Na, and K in the water as a function of density (salinity). As indicated in Figure 7, the water chemistry of Bocana de Virrila reflected evaporation-mineral precipation variations very well. Initially, concentrations of all elements increase with increased salinity. However, with precipitation of $CaCO_3$ and $CaSO_4 \cdot 2H_2O$, the Ca concentration declined rapidly. Concentrations of the other three elements continued to increase with increased evaporation (salinity) until the point of halite precipitation when Na concentrations in the water decreased, and Mg and K became even more concentrated. We would expect, therefore, that calcium sulfate precipitating in equilibrium with waters of relatively low salinity (e.g. density of approximately 1.12) would contain lower concentrations of co-precipitated Na, Mg, and K than calcium sulfate precipitated at a higher salinity (e.g. at the point of halite precipitation). In other words, a bed of calcium sulfate associated with interbedded carbonates should have concentrations of Na, K, and Mg which are lower than a bed of calcium sulfate interbedded with halite. Similarly, concentrations of Mg and K in halite should increase as the salinity of the water from which the halite precipitated increased. However, the Mg/K ratio should remain about the same until concentrations are reached when precipitation of K and Mg minerals can occur. For example, Holser (1963) found that the Mg/K ratio in brine inclusions in halite remained relatively constant throughout the Permian Wellington Formation of Kansas, although the Mg/Cl and K/Cl ratios increased with increasing salinity due to removal of Cl from the water. These concentration differences should appear between beds of anhydrite or halite which may have formed under different salinity conditions, or within individual beds if salinity of the water changed during deposition of that bed. For example, the concentrations of Mg and K should increase vertically within a halite bed if the salinity of the water at the end of deposition of that bed was greater than the salinity at the beginning.

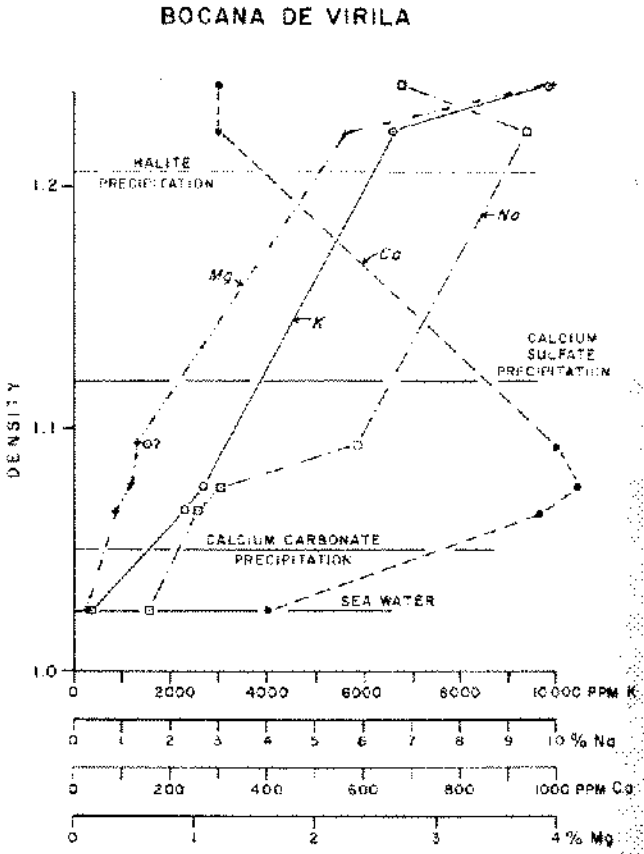

Figure 7. Variations in concentrations of K, Na, Ca, and Mg with density of water from Bocana de Virrila, Peru. Data of Morris and Dickey (1957); densities for initiation of calcium carbonate, calcium sulfate, and halite precipitation estimated from data of Usiglio (1849, *in* Stewart, 1963).

In general, there are no clear variations in mean trace and minor element concentrations in anhydrite or halite beds from either of the two Supai cores which might reflect salinity variations within the depositional basin (Table II). A suggestion of increased salinity during depo-

sition of halite bed IV is indicated by higher mean Mg concentrations in this bed in both cores, although the trend is more pronounced in core 2. In core 1, mean K concentrations also increase upward, but the total variations are small.

Only one bed (halite bed IV) was of sufficient thickness, and sampled in sufficient detail to be able to clearly delineate vertical concentration variations within a single bed. Variations in this 10 m halite bed are best developed in core 2. Figure 8 shows that concentrations of K, Mg, and Ca all increase upward within halite bed IV, whereas Fe remains relatively constant. Mn concentrations (not plotted in Fig. 8) also increase upward. Concentration variations are greatest for Mg, which increases several orders of magnitude from the bottom of the bed to the top. Similar variations, although not as large occur in halite bed II (Appendix, Table A-I). Upward increases in trace and minor element concentrations within beds HIV and HII are interpreted as a record of increasing salinity within the basin during deposition of these beds. We initially expected Ca concentrations to decrease upward within bed HIV because presumably Ca was being removed from the water by precipitation of calcium sulfate somewhere in the basin at the same time that halite IV was being deposited at the sites of cores 1 and 2. However, it is possible that very little contemporaneous calcium sulfate deposition occurred, so that the Ca concentration of the water did increase with increased salinity. In fact, the data of Morris and Dickey (1957) plotted in Figure 7, suggest that after the initiation of halite precipitation, Ca concentrations in the water are constant. With increased salinity (past the concentrations measured by Morris and Dickey), Ca concentrations may actually increase.

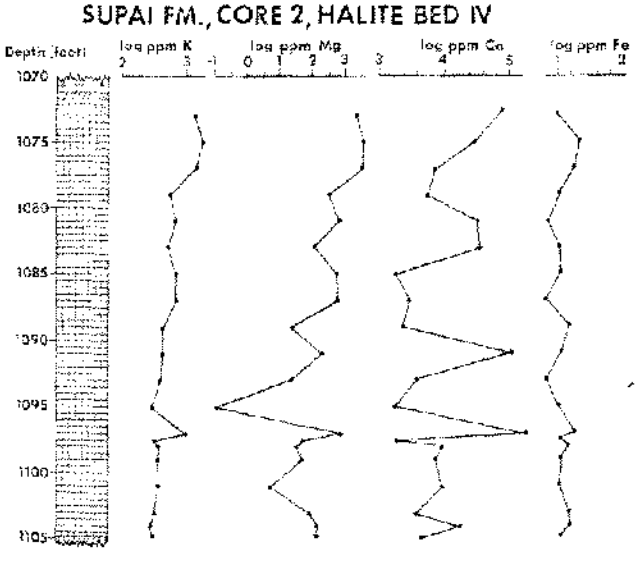

Figure 8. Vertical distribution of logarithmic concentrations of K, Mg, Ca, and Fe in halite bed IV, Core 2 of the Supai Formation (*see* Fig. 3 for location of bed within core).

Variations in Mg and K with salinity are also shown in Figures 9 and 10. In Figure 9 we have plotted Mg vs. K concentrations in the 14 sets of anhydrite analyses listed in Table V. In addition, we have indicated by symbols whether the anhydrite was associated primarily with carbonates (implying lower salinity) or primarily with halite (implying higher salinity). In general, there is a good positive correlation between K and Mg in anhydrite, and all of the anhydrite samples with high Mg and K concentrations are associated with halite, whereas most of the anhydrite samples with low K and Mg concentrations are associated with carbonates.

Figure 10 is a trilinear plot of K, Mg, and Ca concen-

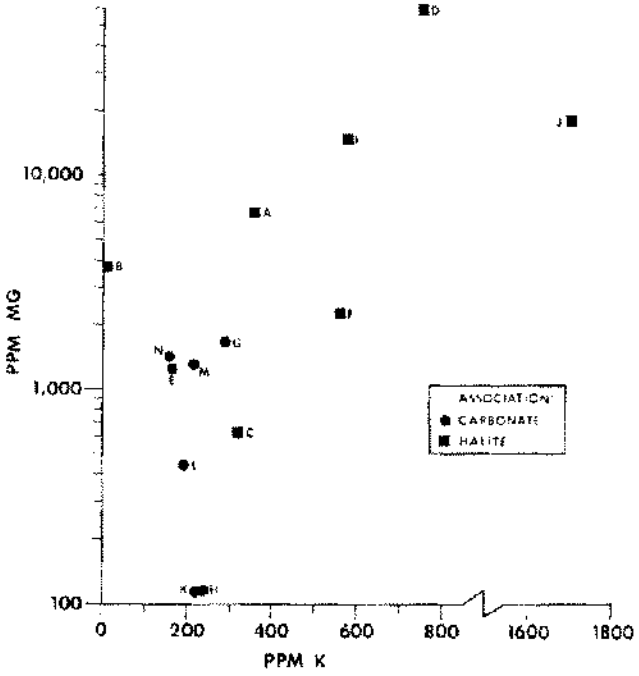

Figure 9. Scatter diagram of Mg and K concentrations in anhydrite samples listed in Table V.

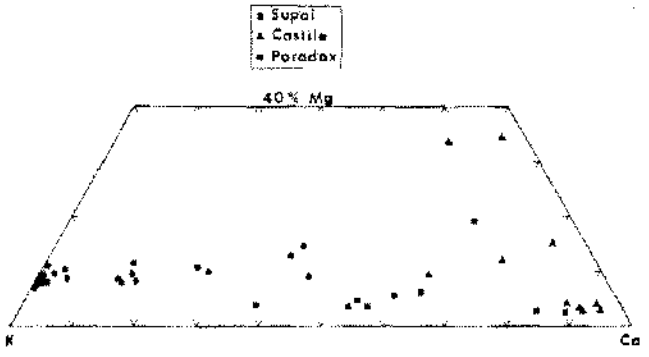

Figure 10. Trilinear plot of K, Ca, and Mg in halite samples from the Paradox Member of the Hermosa Formation and the Halite I Member of the Castile Formation, and mean concentrations in four halite beds in two cores of the Supai Formation. Concentrations are plotted as percent of the sum of K, Ca, and Mg concentrations.

trations in 19 samples from three thin halite beds from the Paradox Member of the Hermosa Formation, in 11 samples from Halite I Member of the Castile Formation, and means of halite analyses in 4 halite beds from two cores of the Supai Formation (Table VI). The analyses from these three different associations fall into relatively distinct groups. The Castile halite samples are all from the oldest halite bed in the Permian evaporite sequence in the Delaware Basin, and represent the lowest salinity association of the three plotted in Figure 10. The Paradox samples are from a halite-potash assemblage and represent the highest salinity association of the three. The Supai halite samples are associated primarily with anhydrite, although the presence of some sylvite and polyhalite suggest that the Supai association is intermediate between the Castile and Paradox associations.

In trying to fit analyses of trace and minor element concentrations in halite and anhydrite to a salinity model we have assumed that the variations in concentrations we measured are indeed a record of variations in water chemistry in the depositional basin. This assumption does not imply necessarily that the minerals we analyzed are primary. For example, it is possible that the anhydrite was deposited as gypsum which was then dehydrated after burial. We are assuming, however, that if there was a gypsum to anhydrite transition, the anhydrite formed retained the trace element signature of the gypsum. If the water released by dehydration of gypsum removed any trace or minor elements, this removal was negligible or at least constant. To those who believe that metamorphism (or metasomatism) of evaporite deposits is universal, this assumption may seem a bit naive. However, the relative constancy of concentrations of all elements analyzed, except Mg, suggest that anhydrite trace and minor element variations are indeed recording variations in these elements within the depositional basin. The extreme variability in Mg concentrations in anhydrite among samples from the same bed, from the same formation, and from different formations is somewhat of a problem. It may be that the Mg variability is indeed measuring Mg variation in basin waters, or Mg variability in pore water during diagenesis, or inclusions of other Mg-rich phases. For example, Dean and Anderson (1974) concluded that variations in Mg concentration in anhydrite from the Castile Formation was due, in part, to variations in minor amounts of dolomite in the anhydrite. Within the Supai Formation, some recrystallization of anhydrite has certainly taken place as evidenced by the presence of polyhalite in several of the anhydrite beds. We tried to avoid polyhalite-bearing anhydrite by selecting samples which appeared pure and showed no polyhalite by X-ray diffraction. However, it is entirely possible that polyhalite, dolomite, or other included mineral phases have caused variability in our analyses. However, the relative uniformity of concentrations of K, Na, Sr, Fe, and Mn suggest that included phases were not a serious problem in our anhydrite analyses.

For halite, the greater variability of trace and minor element concentrations suggests that composition of halite samples may not always reflect water chemistry within the depositional basin. Probably the most serious source of error in halite analyses is caused by variations in the amount and composition of brine inclusions in the halite crystals. It is likely that recrystallization also contributed to variation in halite composition. Compositional variability, especially for halite, points out the danger of making general conclusions regarding depositional conditions for an entire formation based on one or two analyses. Certainly the broad sweeping conclusions on the constancy of ion ratios in seawater since the Cambrian, made by Moore (1971) on the basis of 5 halite analyses from evaporite deposits of different ages, are dangerous.

Conclusions about water chemistry of the depositional basin recorded by trace and minor element compositions of minerals would be most valid if we could be sure that the elements were in equilibrium solid solution within the crystal structure. In anhydrite samples, it is probably safe to assume that most of the Mg and Sr is in true solid solution for Ca. The high positive correlations among Mg, Mn, and Fe suggest that Mn and Fe are also in solid solution for Ca. Table VII shows that Fe^{++}, Mn^{++}, and Mg^{++} have ionic radii slightly smaller than the ionic radius of Ca^{++}. Sr^{++} has a slightly larger ionic radius than Ca^{++} but not significantly larger to prevent limited solid solution. In addition, all four ions (Fe^{++}, Mn^{++}, Mg^{++}, and Sr^{++}) have the same charge as Ca^{++}. We would therefore expect a fair amount of substitution of these four ions for Ca^{++} in the anhydrite structure. It is somewhat puzzling that the Supai anhydrite samples do not show a correlation between Sr and either Mg or Mn although Sr does have a weak correlation with Fe. Na^{+} also has an ionic radius close to that of Ca^{++} but has a different charge. However, because of the abundance of Na^{+} in solution, and its similar ionic radius, we should expect some substitution of Na^{+} for Ca^{++}. K^{+} has both a different charge and a considerably larger ionic radius than

TABLE VII

Ionic radii and electronegativities of 7 ions described as trace and minor elements in this report.

Ion	Ionic Radius (Å)	Electronegativity (relative units)
Na^{+}	0.95	0.9
K^{+}	1.33	0.8
Mg^{++}	0.65	1.2
Ca^{++}	0.99	1.0
Sr^{++}	1.13	1.0
Mn^{++}	0.80	1.5
Fe^{++}	0.80	1.8

Ca^{++} so we would not expect much substitution of K^{+} for Ca^{++}. However, the strong positive correlations between, K, Mg, and Mn concentrations in Supai Anhydrite samples suggest that this substitution does occur. Of the elements discussed, K, Na, Mg, and Ca are transported mainly as ions in true solution. Most of the Fe and much of the Mn transported by streams is carried as detrital grain coatings, by adsorption onto organic matter and clay minerals, and as colloidal oxides and hydroxides. Most of these forms of Fe and Mn would be precipitated leaving some Fe and Mn in true solution. Some Fe and Mn in our analyses may be present as included organic matter, detrital material, or Fe and Mn oxides and hydroxides, but most is probably in crystal structures.

CONCLUSIONS

1. Anhydrite samples from the Supai Formation contain higher concentrations of Mg, Mn, Fe, and Sr than halite samples; concentrations of K are about the same in both minerals. Mg is the most variable of the elements analyzed, both within cores and between cores.

2. In general, there are no significant differences in trace and minor element concentrations within correlative beds in the two cores studied, probably because of the close proximity of the two cores. There are few significant differences in trace and minor element concentrations between beds of the same lithology within cores which might be useful in identifying trace element marker beds for stratigraphic correlation. However, ranking mean concentrations of Mn and Fe in anhydrite beds, and mean Ca concentrations in halite beds in each core provides reliable correlations between the two cores.

3. The most significant interelement correlations are between K, Mg, and Mn in halite, and K, Mg, Mn, and Fe in anhydrite. Most interelement correlations in anhydrite are improved by logarithmic transforms suggesting that trace element incorporation processes are linear for halite and non-linear for anhydrite.

4. Concentrations of trace and minor elements analyzed in Supai anhydrite and halite samples are within the ranges of analyses of other anhydrite and halite samples reported here. However, Supai anhydrite tends to be enriched in all elements measured, relative to the other anhydrite analyses. In general Sr, Na, and K concentrations in anhydrite are relatively constant, varying within an order of magnitude. Mg is the most variable element measured in both anhydrite and halite, varying as much as 3 orders of magnitude among samples from the same bed, the same formation, and different formations.

5. There are few clear vertical variations in trace and minor element concentrations in either core which can be related to changes in salinity within the depositional basin with time. However, one thick halite bed (HIV) shows pronounced upward increases in K, Mg, Ca, and Mn which are interpreted as indicating an increase in salinity within the basin during deposition of this bed. We have concluded that detailed analyses of salt deposits for several elements, especially K and Mg, may yield valuable information about lateral and vertical changes in water chemistry during deposition, and may prove useful in locating zones for potash exploration.

ACKNOWLEDGMENTS

Core samples and lithologic descriptions of the two Supai cores were provided by Edward C. Beaumont through the University of New Mexico. We would also like to thank Douglas W. Kirkland who provided the halite samples from the Paradox Member of the Hermosa Formation, and many of the anhydrite samples whose analyses appear in Table V.

REFERENCES

Anderson, R. Y., Dean, W. E., Jr., Kirkland, D. W., and Snider, H. I., 1972, Permian Castile varved evaporite sequence, West Texas and New Mexico: *Geol. Soc. Am. Bull.*, 83, 59–86.

Dean, W. E., and Anderson, R. Y., 1974, Trace and minor element variations in the Permian Castile Formation, Delaware Basin, Texas and New Mexico, revealed by varve calibration: *in Fourth International Symposium on Salt*, Northern Ohio Geol. Soc., Inc., Cleveland, Ohio (this volume).

Holser, W. T., 1963, Chemistry of brine inclusions in Permian salt from Hutchinson, Kansas: *in Symposium on Salt*, Northern Ohio Geol. Soc., Inc., Cleveland, Ohio, p. 86–95.

Moore, G. W., 1960, Origin and chemical composition of evaporite deposits: U.S. Geol. Survey open-file report.

_____, 1971, Geologic significance of the minor-element composition of marine salt deposits: *Econ. Geol.*, 66:187–191.

Morris, R. C., and Dickey, P. A., 1957, Modern evaporite deposition in Peru: *Am. Assoc. Petrol. Geol. Bull.*, 41:2467–2474.

Peirce, H. W., and Gerrard, T. A., 1966, Evaporite deposits of the Permian Holbrook Basin, Arizona: *in* Rau, J. L., ed., *Second Symposium on Salt*, Northern Ohio Geol. Soc., Inc., Cleveland Ohio, p. 1–10.

Stewart, F. H., 1963, Data of geochemistry, Chapter Y, Marine evaporites: *U.S. Geol. Survey Prof. Paper* 440–Y:53 p.

Winters, S. S., 1963, Supai Formation (Permian) of eastern Arizona: *Geol. Soc. Am. Mem.* 89:99 p.

TABLE A-I

Analyses of trace and minor elements in anhydrite and halite samples from two cores of the Supai Formation. Ca concentrations in percent, all others in parts per million (ppm). Zeros in the Sr column indicate concentrations < 100 ppm; zeros in Mg column indicate concentrations < 0.1 ppm. (see Figure 3 for locations of beds within two cores).

ANHYDRITE

BED CORE–DEPTH(FT)	K	MG	MN	FE	SR	NA
A-XI						
2-1041'6"	187.	1411.	6.6	106.	1048.	3256.
2-1042'	221.	553.	5.0	131.	2918.	6131.
2-1043'	216.	5020.	24.1	110.	2209.	1807.
2-1073'	237.	400.	4.5	100.	1000.	500.
A-X						
2-1105'T	228.	300.	6.0	145.	1250.	350.
2-1105'M	245.	200.	6.0	85.	1250.	280.
2-1105'B	305.	407.	6.6	203.	1087.	589.
2-1117'6"	260.	600.	6.5	196.	1000.	350.
A-IX						
2-1137'	226.	201.	6.0	126.	986.	1328.
2-1138'	223	6592.	6.1	107.	1045.	1268.
2-1139'	207.	2520.	9.1	232.	818.	3024.
2-1140'	539.	41820.	229.5	473.	691.	2053.
2-1141'	276.	2610.	17.6	191.	924.	351.
2-1141'4"	463.	29532.	145.1	545.	805.	306.
2-1142'	237.	2873.	20.2	187.	776.	1109.
2-1142'6"	187.	605.	9.1	202.	907.	1462.
A-VIII						
2-1174'6"	237.	2150.	40.0	85.	700.	4100.
2-1175'	862.	7299.	92.0	1264.	1126.	713.
A-VII						
2-1232'	348.	5215.	24.5	904.	1084.	818.
2-1232'3"	419.	6108.	28.5	808.	994.	621.
2-1232'6"	594.	10684.	29.4	1870.	972.	299.
2-1233'4"	251.	1002.	11.0	200.	912.	281.
A-IV						
2-1307'	249.	203.	9.1	167.	974.	994.
2-1308'	304.	11546.	107.4	206.	924.	1757.
2-1309'	221.	3514.	35.1	196.	864.	2289.
2-1311'	352.	15051.	158.1	286.	704.	3418.
A-III						
2-1343'	345.	5464.	12.4	660.	6619.	1340.
2-1344'	373.	7521.	16.6	835.	1141.	2853.
2-1345'	393.	10460.	22.5	1020.	973.	1381.
2-1346'	260.	4684.	21.9	412.	896.	1171.
2-1347'	304.	5504.	24.2	561.	916.	1235.
2-1348'	353.	16360.	7.7	527.	890.	1943.
2-1349'	332.	9894.	57.7	475.	918.	2857.
2-1350'	318.	4536.	15.5	505.	887.	1196.
2-1351'	746.	15482.	41.9	2523.	7383.	1376.
A-II						
2-1364'6"	262.	956.	5.0	191.	2968.	352.
2-1365'	605.	24725.	129.1	1264.	2203.	385.
A-I						
2-1413'	312.	965.	9.1	218.	945.	2288.
2-1415'	295.	2722.	21.7	252.	1280.	1069.
2-1416'	292.	4057.	20.8	243.	1187.	1298.
2-1416'3"	367.	4847.	30.6	398.	990.	2327.
2-1417'	269.	6897.	43.1	198.	781.	1623.
2-1418'	295.	6640.	40.2	156.	755.	2213.
2-1419'	311.	4949.	39.4	237.	990.	2395.
2-1420'	265.	1414.	16.7	232.	859.	1394.
2-1422'	295.	2033.	55.9	173.	864.	1067.
2-1423'	1578.	23511.	329.7	300.	196.	6771.
A-XI						
1-818'6"	250.	1426.	8.7	255.	4073.	1253.
1-818'10"	257.	956.	6.5	111.	4276.	1660.

ANHYDRITE (Continued)

BED CORE–DEPTH(FT)	K	MG	MN	FE	SR	NA
A-XI (Continued)						
1-819'1"	174.	1406.	13.1	110.	753.	3494.
1-820'4"	339.	5901.	15.5	590.	3054.	1191.
A-X						
1-880'3"	362.	1501.	10.4	399.	3416.	352.
1-883'7"	324.	4262.	15.1	499.	2235.	1060.
1-894'	190.	550.	9.0	50.	650.	2350.
A-IX						
1-913'	4060.	65000.	620.0	8500.	820.	2160.
A-VIII						
1-950'6"	248.	2705.	44.1	251.	500.	2806.
1-951'	571.	11831.	169.8	700.	1082.	556.
A-VII						
1-1007'	405.	9356.	40.5	1227.	2495.	936.
1-1008'	269.	507.	27.4	568.	1364.	355.
1-1009'	519.	12474.	31.2	1874.	2340.	418.
A-VI						
1-1035'	305.	1423.	10.2	356.	1087.	636.
1-1036'	373.	1534.	14.8	327.	1063.	511.
A-V						
1-1045'	245.	1440.	15.0	215.	880.	1050.
1-1045'6"	385.	9896.	17.7	1208.	1006.	741.
A-IV						
1-1094'	390.	14796.	242.3	357.	827.	1837.
1-1095'	322.	5382.	65.4	211.	734.	1016.
1-1098'	346.	21169.	277.7	277.	1008.	1139.
1-1099'	242.	556.	9.1	253.	808.	1081.
A-III						
1-1127'9"	388.	4312.	13.3	560.	901.	1283.
1-1130'	354.	4150.	19.6	1286.	922.	1281.
1-1131'	340.	4218.	12.3	638.	1049.	1235.
1-1132'	186.	956.	10.1	211.	855.	2314.
1-1134'7"	265.	6092.	38.2	402.	978.	1120.
1-1136'10"	234.	2134.	13.7	417.	874.	2114.
1-1138'	271.	3681.	31.7	435.	920.	1227.
1-1139'3"	973.	18349.	44.7	2236.	1089.	1778.
A-I						
1-1193'	292.	3421.	44.3	563.	966.	1207.
1-1196'	267.	9557.	56.3	231.	866.	4628.
1-1197'	337.	1409.	13.1	226.	946.	6640.
1-1199'	288.	3232.	39.4	222.	1010.	1919.
1-1200'	525.	35491.	249.6	887.	992.	1931.

HALITE

BED CORE–DEPTH(FT)	K	MG	MN	FE	SR	CA
H-IV						
2-1073'3"	1317.	2333.	7.1	10.0	0.	7.94
2-1075'	1742.	3484.	10.0	14.5	0.	2.90
2-1077'	1556.	3085.	9.5	13.4	0.	0.66
2-1079'	552.	392.	2.3	10.3	0.	0.57
2-1081'	683.	663.	2.0	8.7	0.	3.18
2-1081B	904.	1188.	3.9	11.6	0.	0.45
2-1083'	523.	111.	1.4	10.1	173.	3.48
2-1085'	664.	580.	2.0	10.5	0.	0.18
2-1087'	708	606.	3.3	8.3	0.	0.30
2-1089'	446.	24.	1.0	12.3	0.	0.46
2-1091'	455.	191.	1.8	10.6	250.	11.33
2-1093'	402.	23.	1.0	8.1	0.	0.35

TABLE A-I (Continued)

HALITE (Continued)

BED CORE–DEPTH(FT)	K	MG	MN	FE	SR	CA
H-IV (Continued)						
2-1095'	290.	0.	0.7	10.2	0.	0.18
2-1097'	1053.	681.	2.1	18.2	688.	16.98
2-1097'6	350.	46.	1.0	10.2	0.	0.19
2-1098'	362.	36.	1.3	12.2	0.	0.92
2-1099'	356.	40.	1.5	10.2	0.	0.67
2-1101'	378.	5.	1.1	10.1	0.	0.87
2-1103'	331.	58.	1.3	12.4	0.	0.37
2-1104'	315.	146.	1.8	12.4	0.	1.76
2-1104'9"	337.	119.	1.0	10.1	0.	0.40
H-III						
2-1117'6"	309.	27.	1.8	10.1	0.	0.54
2-1118'6"	260.	14.	0.5	8.0	0.	0.30
2-1119'	321.	13.	1.1	10.2	0.	0.40
2-1119'6"	350.	6.	1.2	14.3	0.	0.32
2-1120'	337.	22.	1.0	10.1	0.	0.34
H-II						
2-1167'3"	199.	20.	1.3	10.2	0.	0.47
2-1167'6"	405.	28.	1.4	17.7	0.	2.08
2-1168'	311.	32.	1.0	12.1	0.	0.44
2-1168'6"	451.	18.	1.3	14.0	0.	0.15
2-1169'	385.	20.	1.8	17.5	0.	0.72
2-1169'6"	446.	9.	1.5	10.1	0.	0.52
2-1170'	366.	23.	2.8	13.5	620.	18.02
2-1170'6"	252.	2.	1.1	10.3	0.	0.69
2-1171'	227.	5.	1.3	14.8	540.	10.58
2-1171'6"	207.	0.	1.3	10.3	100.	3.29
2-1172'	481.	9.	2.5	12.0	0.	0.76
2-1172'6"	400.	0.	1.2	12.0	0.	0.15
2-1173'	425.	0.	1.5	17.5	0.	0.39
2-1173'6"	389.	0.	1.8	14.2	0.	2.07
2-1173'9"	256.	3.	1.5	14.3	0.	3.94
H-I						
2-1250'	454.	7.	1.2	14.1	0.	0.41
2-1256'	378.	0.	2.2	14.1	0.	0.31
2-1257'	483.	14.	2.8	20.9	0.	0.15
2-1258'	474.	52.	5.5	19.0	0.	0.40

HALITE (Continued)

BED CORE–DEPTH(FT)	K	MG	MN	FE	SR	CA
H-I (Continued)						
2-1260'	515.	21.	2.6	14.2	0.	0.39
2-1261'	513.	29.	2.0	10.1	0.	0.28
2-1262'	487.	4.	2.0	16.6	0.	0.23
H-IV						
1-855'	465.	22.	0.8	12.1	0.	0.75
1-859'6"	416.	48.	0.1	10.1	0.	0.47
1-861'	466.	138.	1.4	12.0	0.	0.28
1-865'	455.	170.	1.2	12.1	0.	0.64
1-867'	452.	54.	1.5	4.6	0.	0.75
1-869'	430.	112.	1.2	10.2	0.	0.18
1-871'	285.	17.	0.9	10.4	150.	1.24
1-873'	323.	0.	0.9	12.4	0.	0.45
1-875'	442.	40.	1.7	14.0	0.	3.91
1-877'	450.	48.	1.5	12.0	0.	0.51
1-878'	385.	39.	1.0	12.3	0.	0.28
1-879'	305.	19.	0.8	10.0	0.	0.43
H-III						
1-895'	354.	15.	0.8	10.1	0.	0.08
1-896'	321.	36.	0.9	10.2	0.	1.03
1-897'	293.	23.	1.0	10.2	0.	0.16
H-II						
1-945'6"	327.	102.	0.8	13.8	0.	0.20
1-946'	349.	8.	0.5	10.2	0.	0.26
1-946'6"	305.	15.	1.0	10.0	0.	0.33
1-947'	343.	0.	0.9	10.2	0.	1.12
1-947'6"	279.	0.	0.9	10.3	0.	0.53
1-948'	261.	0.	0.9	8.1	0.	0.91
1-948'6"	308.	0.	1.5	10.8	0.	6.91
1-949'	285.	1.	1.2	10.5	0.	3.69
1-949'6"	166.	0.	0.8	10.1	0.	0.58
H-I						
1-1036'	313.	40.	0.8	8.0	0.	0.13
1-1038'	306.	10.	1.3	10.2	0.	1.12
1-1040'	346.	24.	0.9	10.1	0.	0.31
1-1042'	313.	0.	0.5	10.0	0.	0.16
1-1044'	240.	0.	0.7	10.0	0.	0.31
1-1045'	335.	7.	0.8	12.0	0.	0.48